

Experimental Investigation of PCM based Round Pin-Fin Heat Sinks for Thermal Management of Electronics: Effect of Pin-Fin Diameter

Adeel Arshad¹, Hafiz Muhammad Ali^{2,*}, Shahab Khushnood², Mark Jabbal¹

¹Fluids & Thermal Engineering (FLUTE) Research Group, Faculty of Engineering, University of Nottingham, Nottingham NG7 2RD, UK

²Department of Mechanical Engineering, University of Engineering and Technology, Taxila, Pakistan

* h.m.ali@uettaxila.edu.pk

Abstract

This experimental study presents the parametric analysis for the round pin-finned heat sinks subjected to steady heat densities for effective and reliable cooling of mobile electronic devices. Phase change material (PCM) namely paraffin wax is adopted as energy storage material and aluminum made round pin-fins are selected as thermal conductivity enhancers (TCEs). A constant volume fraction of 9% of round pin-fins is selected with pin diameter of $2mm$, $3mm$ and $4mm$ and input heat flux was provided from $1.6kW/m^2$ to $3.2kW/m^2$ with an increment of $0.4kW/m^2$. Three volume fractions of $\psi = 0.0$, $\psi = 0.5$ and $\psi = 1.0$ of PCM amount are poured in each configuration of pin-finned heat sinks. A heat sink with no fin is chosen as a reference heat sink to quantify the effect of PCM and TCEs. The thermal performance of PCM filled heat sinks are analyzed to explore the effect of volumetric fractions of PCM, heat densities, pin diameter on latent heat phase, enhancement in operation time, heat capacity and thermal conductance. Three reference set point temperatures (SPTs) are chosen and results have evidenced that a $3mm$ pin diameter heat sink has best thermal performance.

Key words:

Round pin-fin, Heat Sink, Phase Change Material, Thermal Conductivity Enhancers, Paraffin Wax, set point temperatures, Enhancement Ratio, Heat capacity, Thermal Conductance

Nomenclature

TM	Thermal Management
TCE	Thermal Conductivity Enhancer
SPT	Set Point Temperature
T	Thermocouples inside the PCM
W	Thermocouples inside the side walls
H	Thermocouples inside the base
HSU	Heat Storage Unit
PCM	Phase Change Material
V_S	Total Volume of Heat Sink
V_f	Total Volume of fins
t_{cr}	Time to reach for a critical temperature
G	Thermal conductance
Q	Heat Transferred
ΔT	Temperature difference
T_{max}	Maximum temperature after charging phase.
T_{amb}	Temperature at ambient condition.
q	Heat Flux
c_{PCM}	Specific heat
T_m	Melting Temperature of PCM

Greek Symbols

γ	Volume fraction of the TCE
ψ	Volumetric fraction of PCM
v_{PCM}	Specific volume of PCM
ξ	Enhancement ratio at TCE
ε	Enhancement ratio at PCM
c	Heat Capacity
κ_{PCM}	Thermal Conductivity of PCM
λ_{PCM}	Latent Heat
ρ_{PCM}	Density of PCM

1-Introduction

Due to advancement of modern electronic packages, heat transfer augmentation technologies are needed to be improved for reliability of these modern packages. Consequently, various advance heat transfer techniques have been introduced for the cooling of electronic devices which may contain active and passive cooling. Heat, which is the main byproduct of any electronic device, generates inside the miniature and complex circuits of these devices. The key objective of a heat transfer augmentation technique is to enhance the thermal performance of system by enhancing the coefficient of heat transfer. Although, there are some typical cooling techniques like piezoelectric pump, air cooling, liquid cooling and heat pipes which remove heat efficiently [1, 2]. However, latent heat thermal energy storage system (LHTESS) is now highly under research for passive cooling of electronic devices. A LHTESS has a capability to absorb large amount of heat inside it and to reject this heat in surrounding [3, 4]. Phase change materials (PCMs), have the characteristics to absorb high amount of thermal energy during changing the solid-liquid interface [5]. PCMs have a large amount of latent heat of fusion, high specific heat, chemical stability under repeated melting and cooling modes, high volumetric density, little sub-cooling, small volume change, low vapor pressure and are non-toxic, non-explosive and non-flammable [6].

A fewer studies have been reported on parametric investigation of LHTESS. Wang et. al. [7] carried out the numerical parametric investigation of PCM volume fraction, aspect ratio, temperature difference and PCM properties of PCM-based heat sink. The results concluded that a heat sink with PCM has better thermal performance and aspect ratio. Qu et al. [8] conducted the experimental work for passive cooling of electronics using parallel hybrid heat sink saturated with solid copper and pure paraffin wax. The results showed that lower base temperature of heat sink was achieved in case of metal foam-PCM then pure paraffin with a linear trend. Mahrous [9] carried out an experimental study based on PCM based sink and investigated the fins arrangement and number of fins. Heat sinks were partially filled with paraffin wax and effects of heating rates were observed. It was concluded that both heat rate and peak temperature reduced using PCM based heat sinks. The effect of thermal resistant for heat management of electronics using finite element analysis was reported by Grujicic et al. [10]. Authors explored the effect of surface roughness, applied pressure, mechanical and thermal properties for two PCMs and acrylic or

silicon base tapes to cool the central processing unit. The results revealed that the use of thermal interface material lowered the overall base temperature.

Hajmohammadi et. al. [11] carried out the numerical study of V-shaped fins/inserts embedded in a square heat generating cavity. The authors performed the geometric optimization of fins and concluded that V-shaped inserts had the remarkable heat transfer performance and reduced the base temperature of heat generating cavity. Further, to improve the cooling performance, Hajmohammadi et. al. [12, 13] presented the numerical study of forced convection cooling and proposed the correlation between the thick plate and heat source. Authors concluded that at low Reynolds number and low Prandtl number, temperature was reduced with the interface of plate. Hajmohammadi and his co-authors [14, 15] presented the numerical investigations of laminar forced convection cooling of plate and round pipe under the array of heat sources of varying size of spacing. Najafi et. al. [16] carried out the optimization study of plate and fin heat exchanger using genetic algorithm using air as a working fluid at both end of heat exchanger.

For PCM-based finned heat sinks for thermal management of electronic devices with a constant volume fraction of 9% of fins, an experimental study was carried out by Baby and Balaji [17]. An enhancement ratio of 18 was obtained for *pin-fin* heat sink and it was concluded that *pin-fin* heat sink had better efficiency than plate-fin heat sink filled with PCM. In extension of phase change cooling of electronic devices, Baby and Balaji [18] performed an optimization study by choosing three different volume fractions (4%, 9% and 15%) of *pin-fins*. The authors concluded that a *pin-fin* heat sink of volume fraction of 9% had the best thermal performance for cooling of portable electronic devices.

Jaworski [19] reported a numerical study using round *pin-fin* heat spreader filled with PCM. Heat transfer rates and thermal resistance were investigated under steady state conditions. The conclusions revealed that the use of PCM was effective in heat transfer through fins. TM of microelectronics using a platform filled with PCMs was investigated using experimental, numerical and analytical approaches by Tigner et. al. [20]. The authors concluded that thermal response increased due to the decrease in surface area which transferred heat. An transient heating and cooling phase change cooling of electronics was experimentally carried out by Baby and Balaji [21] using plate-finned PCM filled heat sink. Authors conducted a detailed experimentation on different constant and intermittent heating loads. The results claimed that a plate matrix PCM

based heat sink reduced the base temperature in comfort and reliable temperature conditions in intermittent operation mode.

Sun et, al. [22] proposed a natural cold source with PCMs for cooling of telecommunications base stations of China. Mathematical model and then prototype of a latent heat storage unit was developed. Authors reported that a significant amount of energy was saved by latent heat storage unit to cool the telecommunications base stations. Alshaer and his co-authors [23, 24] carried out the numerical studies for phase change cooling of electronics using carbon foam/PCM/carbon nano tubes composite. Authors tested three different modules of pure carbon foam (CF)-20, CF20+RT65 and CF-20+RT65/Nano carbon tubes. It was revealed that RT65 and multiwall carbon nanotubes lead to 11.5% reduction in surface temperature of carbon foam of porosity less than 75%. Thermal performance of composite PCMs were also under observation employing carbon nanofillers in PCM in transient mode by Fan et, al. [25]. Carbon nanotubes and graphene nanoplatelets were used to make composite PCM. The results showed that carbon nanofillers had undesirable results but carbontubes and graphene nanoplatelets had much better thermal performance in transient conditions.

Kalbasi and Salimpour [26] developed and optimized the PCM based rectangular enclosures by changing the geometric parameters. Results revealed that for a rectangular enclosure with vertical fins, it was better to use wider enclosure than a square and thin one. Furthermore, authors concluded that the ratio of vertical fin thickness to horizontal fin had no significant effect. Nada and Alshaer [27] presented a detail parametric numerical study using different carbon foam structures of different porosities and different PCMs. The results showed that with decreasing carbon foam and PCMs thermal conductivities, increasing porosity and module height increased the module temperature. Additionally, it was revealed that transient temperature of module was decreased and time to approach any steady state temperature was delayed of a higher heat of fusion of PCM.

In recent past, Srikanth et, al. [28] presented an experimental and numerical study of *pin-fin* heat sink filled with n-eicosane as a PCM with an objective to increase the charging time during operation and to decrease the discharging time during idle conditions. At constant heat flux and PCM amount, 40 various geometrical configurations of heat sinks were taken. Authors carried out the multi objective optimization using artificial neural network and predicted the optimum

configuration of heat sink. In extension of phase change of cooling, Ahmed et, al. [29] experimentally carried out the TM of tablet computers using two PCM (*n-eicosane* and PT-37) of same melting temperature but different latent heat of fusions. Authors selected two encapsulations of different sizes and same thickness, further examined the effect of angular positions and power densities. A reduction in temperature of 20°C of heat sink was achieved and it was concluded that angular position had no significant effect of PCM melting. Fan et, al. [30] contributed a very promising experimental study based on the PCM based thermal energy storage heat sinks. Two PCMs, liquid metal (Pb-Sn-In-Bi alloy) and an organic PCM (1-octadecanol) having same melting temperature of 60°C were investigated under various power densities. It was revealed that the liquid metal PCM significantly outperformed over the organic PCM not only in extension in heating time also in shorten the cooling period due to higher thermal conductivity of liquid metal.

A numerical study by Sahoo et, al. [31] was proposed for the orthotropic structure composite fins with PCMs and comparison was carried out with isotropic fins. The result found that orthotropic had better thermal performance against isotropic fins, kept the base temperature lower also had the less volume than isotropic fins. Swaminathan Gopalan and Eswaran [32] carried out transient three dimensional numerical study of lattice frame materials and honey comb structures PCMs based heat sinks. Authors explored the parameters of configuration and porosity of porous structure, heat transfer distribution in sensible and latent heating, usage mode of heat sinks under different conditions.

In continue of this, numerical investigation for current models of different brands of nearly similar dimensions was proposed by Thomas et, al. [33]. Authors selected the *n-eicosane* as a PCM, different power levels were provided at heat sink base, effect of power densities and melt fractions were discussed in natural convection conditions. Similarly, Tomizawa et, al. [34] proposed a numerical and experimental study to investigate the various parameters (effect of mass, latent heat, thermal conductivity, configuration of PCM sheet and thermal conductivity of material). Using finite element analysis, optimum dimensions and shape of PCM were defined. The authors concluded with statements that PCM sheet with copper sheet as a thermal conductivity enhancer had better TM for mobile devices.

A very novel technique with porous metal fiber sintered felt (PMFSF) PCM based heat sinks using porous matrix of copper fibers of ample antler microstructure on its surface was examined by

Wang et, al. [35]. A composite of MF-PCM (paraffin/PMFSF) was prepared and three different heat sinks of empty, with paraffin wax and MF-PCM were carried out under observation. Authors concluded that PMFSF showed more enhancement in heat transfer than PCM, further it was evidenced PMFSF had more potential then metal foam. Alimohammadi et, al. [36] performed an experimental study for cooling electronic chips using nano-PCMs under free and forced convection modes. Heat sinks of six different scenarios of simple heat sink, heat sink with PCM and heat sink with nano particles were under tested under steady and transient operations. Authors predicted that temperatures decreased about 14°C and 10.5°C using PCM and nano-PCM both for free and forced convection.

Currently, Gharbi et, al. [37] presented a study of rectangular enclosure heat sinks filled with PCM (plastic paraffin) for continuous and intermittent regimes for discrete heat sources. Authors concluded that thermal performance of heat sink strongly depended on the repetition of heat density, further under intermittent regime, a maximum of lower temperature was achieved for fractionating cycle into 4 to 8 cycles. An multi objective optimization of PCM based heat sink of 72 pins at 4 discrete heating was experimentally carried out by Srikanth and Balaji [38]. Authors adopted the non-dominated sorting genetic algorithm to determine the optimization of parameters of discrete power levels, stretching the charging mode and shortening the discharging mode of heat sink. The results concluded that more multi objective optimization was required for higher discrete power source and type of TCEs. The most recent parametric experimental study based the square fin profile reported by Arshad and his co-authors [39, 40] selected the 9% volume fraction of TCEs and concluded that a 2mm fin thickness had the maximum thermal performance comparing with *no fin*, 1mm and 3mm fin thickness PCM filled heat sinks.

The previous all aforementioned studies clearly explain that a fewer studies have been reported on round *pin-fin* heat sinks for passive cooling of electronics using PCMs as a thermal energy storage material, also none has reported any experimental and numerical study based on parametric investigation with influence of paraffin wax as a PCM. The current study focus on the parametric investigation of fin diameter, amount of PCM (paraffin wax), effect of heat densities for four different configuration of round pin-finned heat sink.

2-Experimental Setup and Procedure

Typical experimental setup used in this research study is shown in Figure 1. Flow diagram in Figure 1, completes the measurement procedure by employing four basics components (DC power supply, PCM filled heat sink assembly, data logger and laptop). A DC power supply (Kaysieght Technologies 6675A, 120V/18A) is used to input the constant heat densities ranging from $1.6kW/m^2$ to $3.2kW/m^2$ with a step of $0.4kW/m^2$. Current and voltage are adjusted using Ohm's law. DC power supply has accuracy of voltage $0.04\% + 120mV$ and current $0.1\% + 12mA$ at reference temperature of $25^\circ C$. Four different configurations of finned heat sink are used as a heat storage unit (HSU), which are no fin heat sink chosen as a reference heat sink for baseline comparisons, three round *pin-fin* heat sinks of $2mm$, $3mm$ and $4mm$ pin diameter having constant volume fractions of $\gamma = 9\%$ as a thermal conductivity enhancers (TECs). The volume fraction of TCEs denoted by γ is calculated using Eq.1, which is actually *the ratio of volume occupied by the fins to the total empty volume of heat sink*.

$$\gamma = \frac{V_{TCE}}{V_S} \quad \text{Eq. 1}$$

In the present research activity, the reason to take the $\gamma = 9\%$ is that earlier Baby and Balaji [18] and recently Arshad and his co-authors [39, 40], and Ashraf et, al. [41] reported that a finned heat sink of TCEs volume fraction of 9% provided the best thermal performance for passive thermal management of portable electronic devices. The heat sinks (*no fin*, $\phi = 3mm$ and $\phi = 4mm$) are machined using computer numerical control (CNC) machine whereas the heat sink of $2mm$ pin diameter is manufactured using electric discharge machine (EDM). A reverse pattern of $\phi = 2mm$ *pin-fin* heat sink is made using copper on wire cut EDM and then die sink EDM is used [42]. The Figure 2 shows the two dimensional projection view of $\phi = 3mm$ *pin-fin* heat sink in actual dimensions. Aluminum ($Al - T6 - 6061$) block is used to made all configurations of heat sinks with overall dimensions of $114 \times 114 \times 25mm^3$. All dimensions of materials required to make HSU are given in Table 1.

Table 1-Dimensions of material used for HSU.

Sr. No.	Materials Used	Dimensions(mm)
1	Perspex sheet	$115 \times 115 \times 5$
2	Silicon Rubber gasket	$115 \times 115 \times 3$ (with a cut out of 114×114)
3	Rubber Pad for heat sink	$220 \times 220 \times 25$ (with a cut out of 114×114)
4	Rubber pad for heat sink bottom	$220 \times 220 \times 65$

Each heat sink (acting a HSU) is filled with phase change material (PCM) namely paraffin wax [43]. Experimentation is carried out at three different volumetric fractions of paraffin wax ($\psi = 0.0, \psi = 0.5$ and $\psi = 1.0$) to investigate the effect of PCM amount for thermal performance of round *pin-fin* heat sinks. Table 2 provides the material properties used in this research activity. The volumetric fraction of PCM denoted by ψ , is calculated using Eq. 2, which is *the ratio of PCM volume to the total volumetric capacity of heat sink*.

$$\psi = \frac{v_{PCM}}{V_S - V_f} \quad \text{Eq. 2}$$

Constant heat densities at the base of HSU is provided through a silicon rubber plate heater (OMEGALUX) of dimension of $100 \times 100 \times 1.14 \text{ mm}^3$ which is attached to heat sink base milled as per dimensions of heater. Heater is made of coil-type nichrome which has a tendency to provide a maximum heat flux of 15.5 kW/m^2 . Data at seventeen different locations of heat sink is measured through high precision K-type thermocouples (Omega, 0.5 mm diameter) and calibration is performed as per ASTM standard [44] for temperature range of $0 - 100^\circ\text{C}$. The maximum variation is found about $\pm 0.1^\circ\text{C}$. A step by step assembly view of different components of heat sink is shown in Figure 3.

Table 2-Thermo-physical properties of materials.

Material	κ_{PCM} (W/mK)	c_{PCM} (kJ/kgK)	λ_{PCM} (kJ/kg)	T_m (°C)	ρ_{PCM} (kg/m ³)
Paraffin Wax	0.167(Liquid)	2.8	173.6	56-58	790(Liquid)
	0.212(Solid)				880(Solid)
Aluminum	202.37	0.871	-	660.37	2719
Rubber Pad	0.043	1.23	-	-	2500

A detail positioning of all thermocouples is shown in Figure 4. The thermocouples denoted by T1-T8 are protruded inside the PCM about 20mm and fixed at different heights from the heat sink base. Thermocouples T1&T6, T2, T5&T8 and T3, T4&T7 are fixed at 10mm, 15mm and 20mm respectively. Whereas W1&W3, W4&W5, and W2&W6 are fixed inside wall of heat sink at 10mm, 15mm and 20mm, respectively. Thermocouples H1, H2 and H3 are inserted in a 1.5mm deep groove at equally distanced to measure the heat sink base temperature. All thermocouples are fixed using Araldite™. A detail of thermocouples inserted inside the paraffin wax and side wall of heat sink is given in Table 3 and 4, respectively.

All the experimentation is carried out at room temperature of 18°C, a thermocouple is kept at working space. Transient temperature variations recorded by thermocouples are taken after 5s interval. HSU assembly is insulated using rubber cork cut in two halves, top surface is covered using silicon gasket and perspex sheet which helps to visualize the melting and cooling fractions of paraffin wax with time. A PC-based data logger (Agilent 334972A) was used by inserting all the thermocouples in multiplexer, which was connected to laptop. Agilent Technologies, Inc. (Taft Ave. Loveland, USA) software is used to record the temperature at interval of 5s as the length of the experiment. The accurate amount of paraffin wax at different volumetric fractions is measured by calibrated mass balance. The range of heat fluxes, provided at the heat sink base was chosen according to normal operating power of hand-held electronic devices.

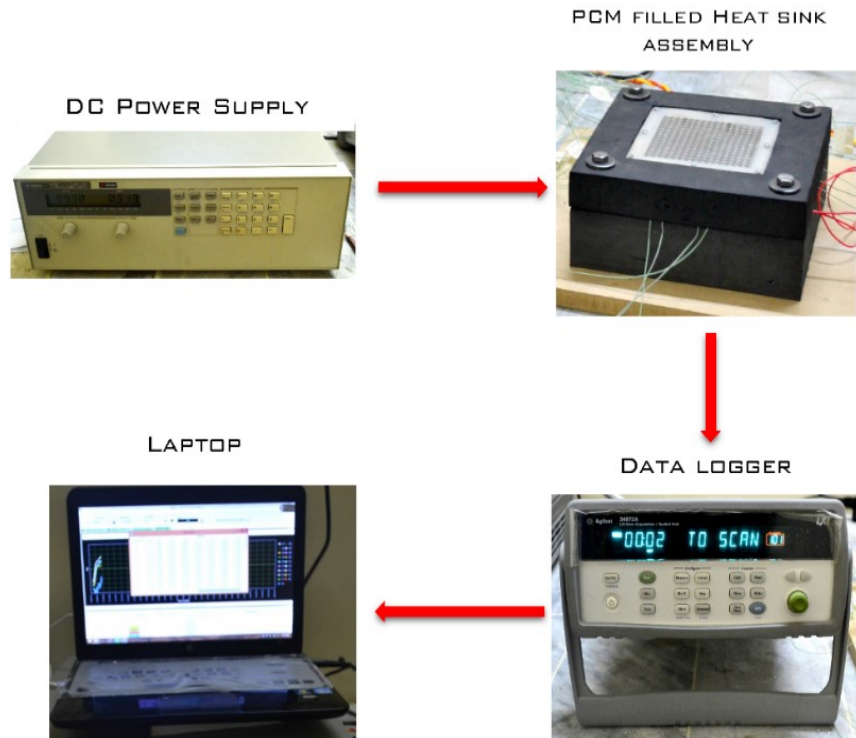


Figure 1-Flow diagram for present experimental HSU.

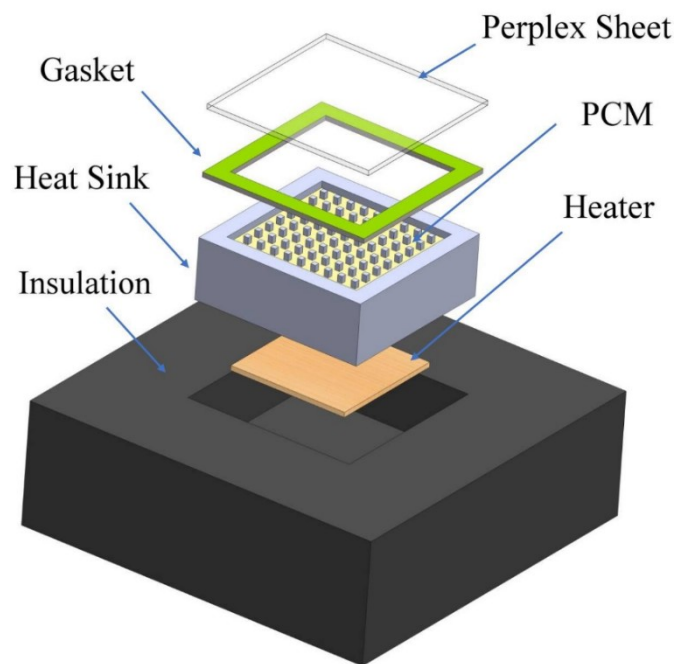


Figure 3-Assembly drawing of PCM based heat sink.

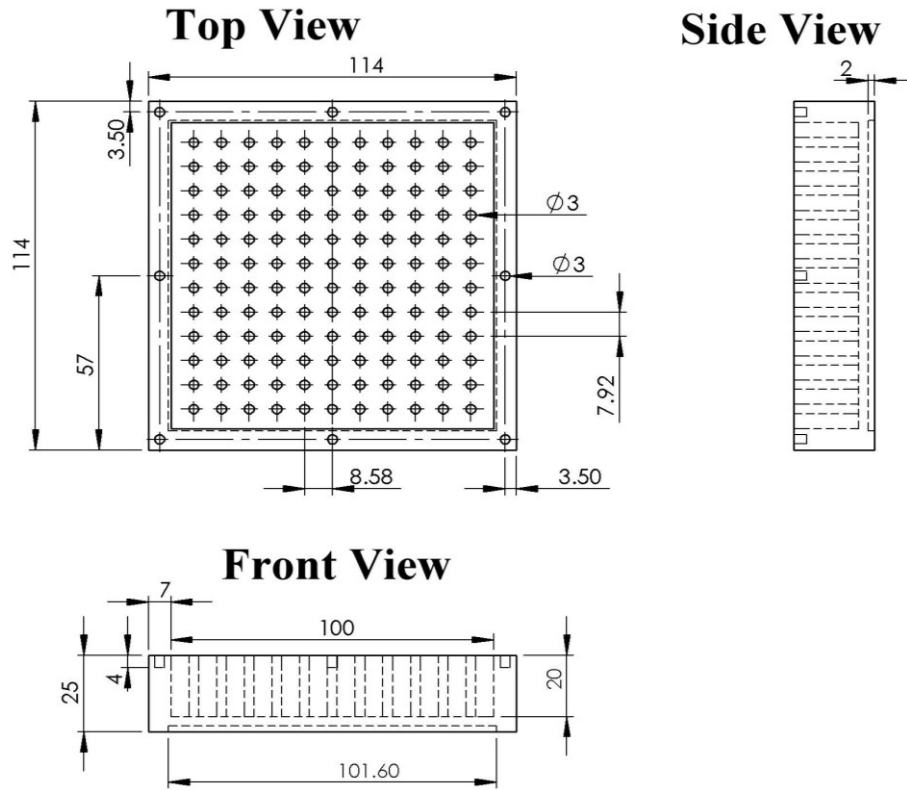


Figure 2- Two dimensional projections of 3mm pin diameter heat sink.

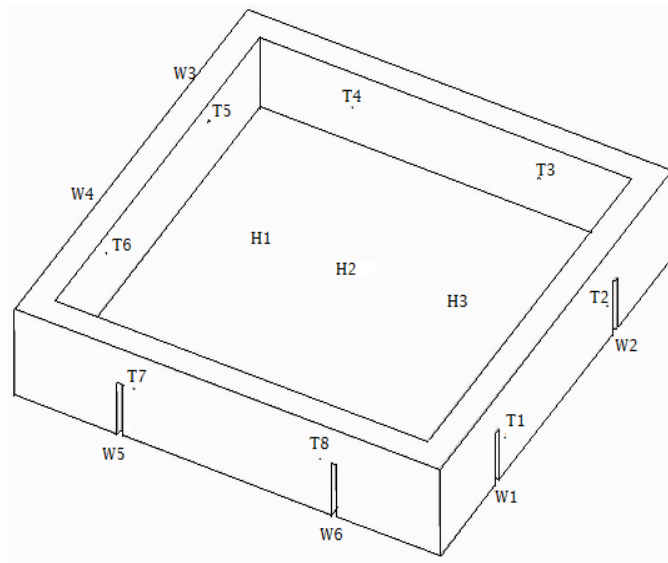


Figure 4-Positoin of thermocouples.

Table 3-Thermocouple positions placed inside the paraffin wax from side walls.

Sr. No.	Type of Heat Sink	Position of thermocouples placed inside the PCM (mm)							
		T1	T2	T3	T4	T5	T6	T7	T8
1	No Fin	32	32	32	32	32	32	32	32
2	$\varphi = 2mm$	41	30	41	30	41	30	41	30
3	$\varphi = 3mm$	41	28	41	28	41	28	41	28
4	$\varphi = 4mm$	40	30	40	30	40	30	40	30

Table 4-Positions of thermocouples located at side walls from side walls.

Sr. No.	Types of Heat Sink	Position of thermocouples placed at the side walls					
		W1	W2	W3	W4	W5	W6
1	No Fin	33	38	33	38	33	38
2	$\varphi = 2mm$	33	38	33	38	33	38
3	$\varphi = 3mm$	33	38	33	38	33	38
4	$\varphi = 4mm$	33	38	33	38	33	38

3-Result and Discussion

3.1-Effect of PCM Volumetric Fractions

The effect of PCM (paraffin wax) volumetric fractions is shown in Figures 5a-5d, input heat flux of $2.4kW/m^2$ is provided at the base of each heat sink (*no fin*, *2mm*, *3mm* and *4mm* pin diameter). Volumetric fractions of paraffin wax are chosen of $\psi = 0.0$, $\psi = 0.5$ and $\psi = 1.0$. Thermocouples inserted inside the heat sink H1, H2 and H3 are chosen to plot the temperature

variation for each configuration of heat sinks. It is seen from Figure 5, that a rapid increase in temperature is obtained at $\psi = 0.0$, which is expected. But at PCM level of $\psi = 0.5$, the base temperature rises lower than $\psi = 0.0$, and further a more lower case is seen for an amount of PCM at $\psi = 1.0$. This ensures that a heat sink either with fins or without fins, a PCM filled at $\psi = 1.0$ has maximum tendency to keep the heat sink base temperature under reliable and comfort temperature limits.

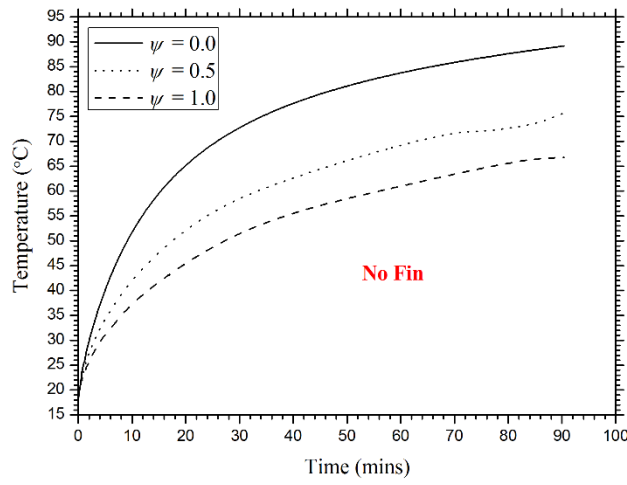


Figure 5(a)

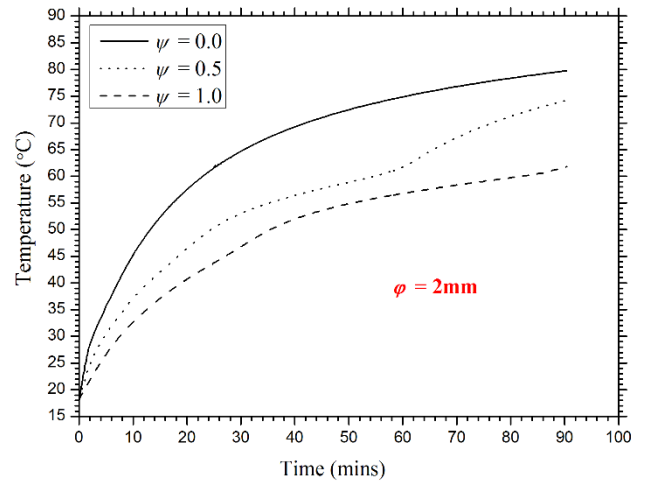


Figure 5(b)

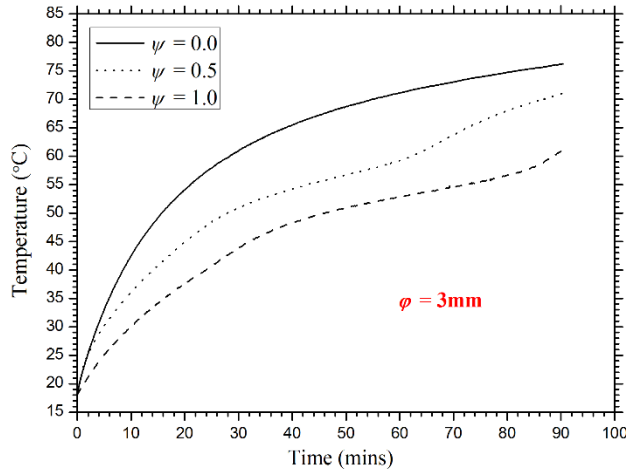


Figure 5(c)

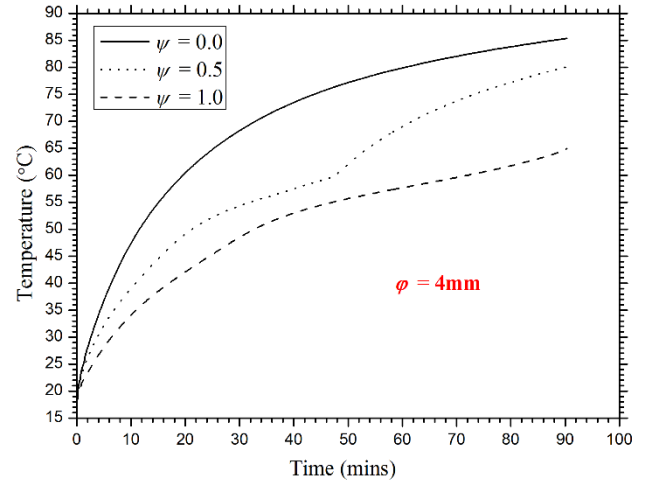


Figure 5(d)

Figure 5- Comparison of heat sinks base temperature at different volumetric fractions of PCM (a) No fin (b) $\phi = 2mm$ (c) $\phi = 3mm$ (d) $\phi = 4mm$

3.2-Effect of Input Heat Flux on Temperature Profile

The effect of different input heat densities is shown in Figure 6 for $2mm$ pin diameter heat sink. A range of heat flux from $1.6kW/m^2$ to $3.2kW/m^2$ is provided at heat sink base through plate heater. Time-temperature profiles are recorded using base thermocouples H1, H2 and H3 at PCM level of $\psi = 1.0$. The Figure 6 shows that the latent heating phase gets shorter as the input heat flux increases, as expected. It is seen that no solid-liquid phase change occurs at $1.6kW/m^2$ even after $140mins$ but a rapid phase change can be seen for $3.2kW/m^2$ input heat density, the phase change occurs just after $28mins$. Further, there is a most significant trend can be seen for latent heating phase completion time.

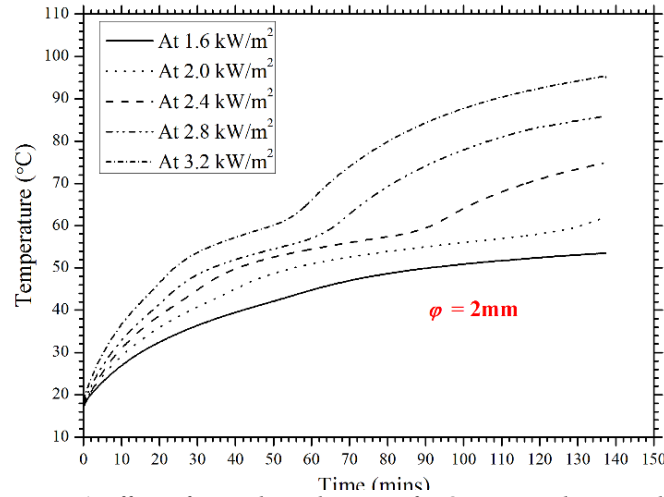


Figure 6-Effect of input heat densities for 2mm pin diameter heat sink.

3.3-Effect of Fin diameter of different Heat Sink Configurations

Figures 7a-7c reflect the effect of pin diameter of a round *pin-fin* heat sink in comparison with no fin heat sink. A heat flux of 2.8 kW/m^2 is provided at the HSU and thermocouples H1, H2 and H3 are used to plot the time-temperature history. Heat sinks of *no fin*, 2mm, 3mm and 4mm pin diameter configurations are filled with three different volumetric fraction ($\psi = 0.0, \psi = 0.5$ and $\psi = 1.0$) of paraffin wax. It is seen that in all cases of ψ , pin diameter of 3mm shows the minimum rise in heat sink base temperature in comparison of *no fin*, 2mm and 4mm pin diameter heat sinks. Latent heating phase duration extends as the amount of PCM doubled as shown in Figures 7b and 7c in cases of finned heat sinks, however an increase in lower base temperature can be evidenced in case of $\phi = 3 \text{ mm}$ also a slight increase in latent heating phase duration can be seen in case of $\phi = 3 \text{ mm}$ at $\psi = 1.0$. A heat sink with lower base temperature and more latent heating phase ensures the best thermal performance to transfer heat in surrounding generated inside compact chips of electronic devices. Furthermore, the variations in temperature profiles of 2mm and 4mm pin diameter is either due to the more number of fins or more pitch distance between the fins. Critically, the reason of the best heat transfer characteristics for the case of 3mm fin diameter heat sink is the optimum number of fins, pitch of fins (the fin spacing in stream-wise, span-wise and diagonal directions). Additionally, the enhanced latent heating phase duration is because of

optimum fins distribution which transfer the internal generated heat more uniformly through fins without causing local overheating the heat sink base.

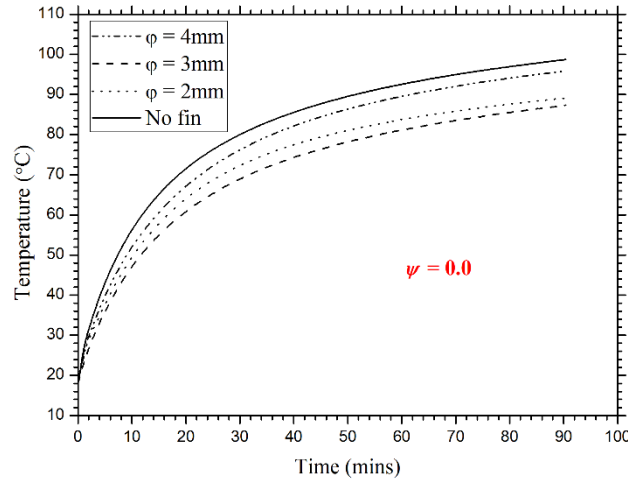


Figure 7(a)

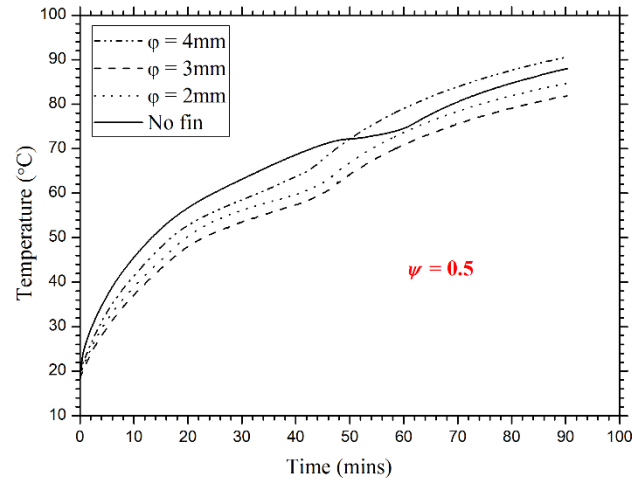


Figure 7(b)

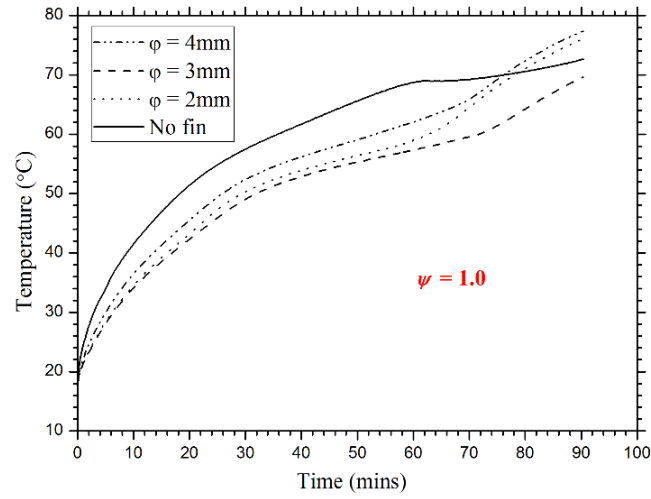


Figure 7(c)

Figure 7- Comparison of fin diameter of different volumetric fractions of PCM at $2.8kW/m^2$ (a) $\psi = 0.0$ (b) $\psi = 0.5$ (c) $\psi = 1.0$

3.4- Temperature variation within PCM for melting and solidification phases.

A complete charging and discharging is shown in Figure 8, for pin diameter of $\phi = 3mm$ paraffin wax filled heat sink. As it is evidenced from Figure 7c, that a $\phi = 3mm$ pin-fin heat sink shows the better thermal performance than all compared finned heat sinks. The complete charging and discharging cycle is subdivided into two regions first one is melting phase and second is cooling phase. Both phases are further labeled into three sub-regions shown in Figure 8. Thermocouples fixed at heat sink base, side wall and inside the paraffin wax are chosen to map the transient variations of phase change temperatures for a complete cycle at input power density of $2.8kW/m^2$.

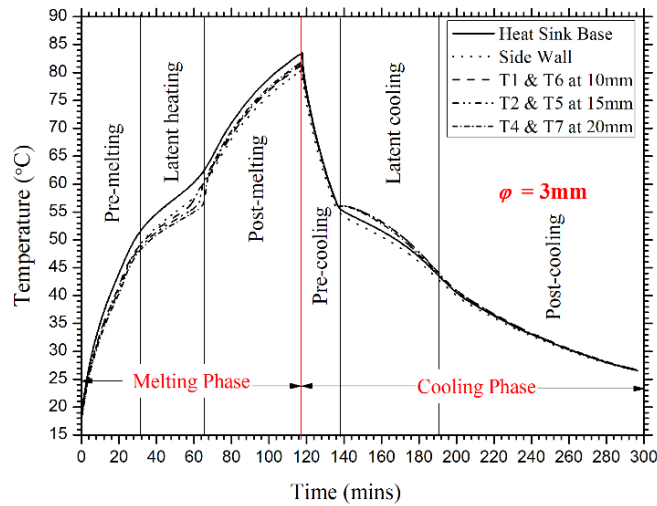


Figure 8-Charging and discharging cycle of $\phi = 3mm$ pin-fin heat sink at $2.8kW/m^2$.

3.5- Temperature uniformity in spatial directions.

The spatial effects of temperature variations inside the paraffin wax at different locations are shown in Figures 9a-9c. Input heat density of $2.8kW/m^2$ is provided at the base of heat sinks and temperature are recorded at 1500s, 3000s, 4500s and 6000s for better graphically represent the melt fraction inside the paraffin wax. Thermocouples at four equally distances are fixed on each heat sink (2mm, 3mm and 4mm pin diameter) for better understanding. An average values of thermocouples H1, H2 and H3 inserted at base, T1&T6 located at height 5mm, T2&T5 located at a height of 10mm and T4&T7 located at a height of 15mm, are taken to map the temperature

distribution in vertical direction of a heat sink. As expected, the thermocouples inserted at heat sink base record higher temperature as they are directly in contact with plate heater. However, temperature variations inside the paraffin wax are so significantly abrupt and a uniformity which is due to the natural convection heat transfer can be seen for each configuration of *pin-fin* heat sink at specific time.

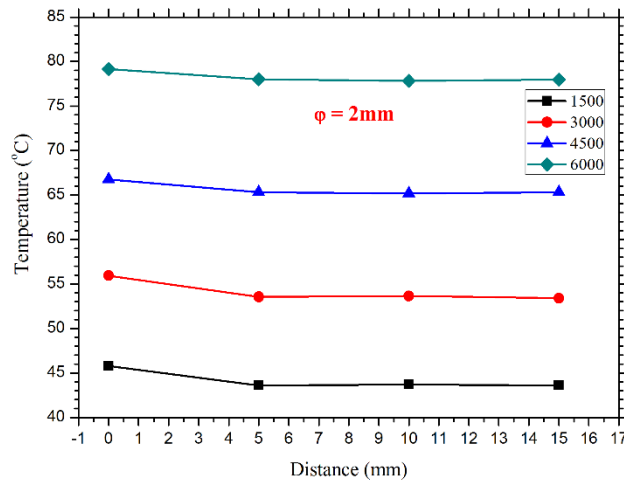


Figure-9(a)

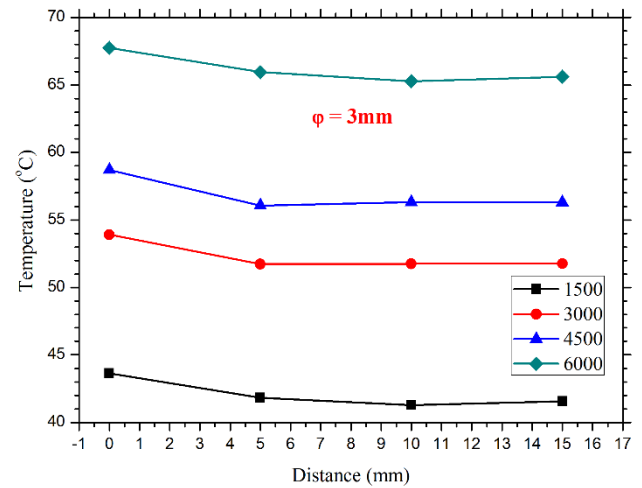


Figure-9(b)

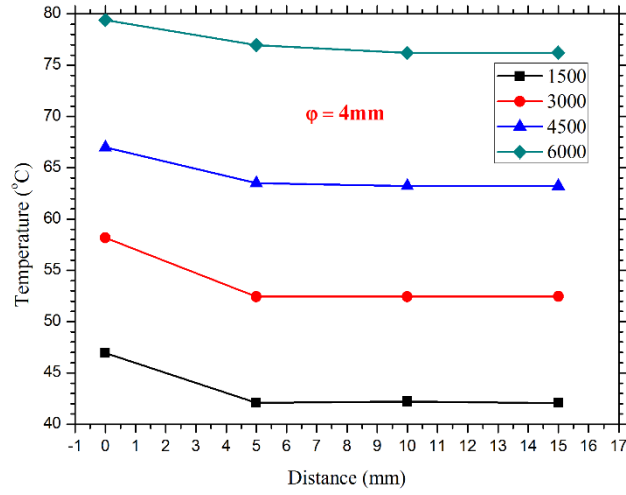


Figure-9(c)

Figure 9- Temperature variations in spatial directions at 2.8 kW/m^2 (a) $\phi = 2\text{mm}$ (b) $\phi = 3\text{mm}$ (c) $\phi = 4\text{mm}$

3.6-Operation time enhancement of different configurations of heat sinks for critical SPTs

To ensure the thermal performance of different configurations of *pin-fin* heat sinks tested in this study, enhancement in operation time is presented for three different critical SPTs (i.e. 60°C , 65°C and 70°C). Bar charts shown in Figure 10a-10b, represent the time taken by the finned heat sinks of various pin diameters to reach the critical SPTs of 60°C and 70°C . A complete summary of time to reach critical SPTs is given in Table 5 for heat flux range of 2.0 kW/m^2 to 3.2 kW/m^2 at $\psi = 1.0$ volumetric fraction of paraffin wax. Average reading values of thermocouples of H1, H2 and H3 are taken. The critical SPTs chosen are actually the maximum design temperature limit for any portable electronic gadgets at which it can't lose its functionalities and reliability. It is evident from Figure 10a-10b that a PCM filled *pin-fin* heat sink of $\phi = 3\text{mm}$ takes maximum time to reach SPTs of either 60°C or 70°C in comparison of other PCM filled heat sinks. The time to reach SPT of 60°C is recorded around 172 mins at 2.0 kW/m^2 and around 61 mins at 3.2 kW/m^2 input heat fluxes for 3mm pin diameter PCM filled heat sink. Similarly, for SPT of 70°C , for the case of $\phi = 3\text{mm}$, it is noted around 80 mins and 130 mins at input heat flux of 3.2 kW/m^2 and of 2.4 kW/m^2 respectively. This reveals that a $\phi = 3\text{mm}$ round *pin-fin* PCM filled heat sink has best thermal performance for passive cooling of hand-held electronic devices under reliable and comfort temperature limits. Additionally, a closer look in case of *no fin*, $\phi = 2\text{mm}$ and $\phi = 4\text{mm}$ depicts

another picture of coin, the variation in time to reach either 60°C or 70°C is due to the local overheating occurring between the layers of paraffin wax which don't transfer heat to adjacent layer. This results the rapid rise in base temperature instead of keeping lower.

As it is evident that $\varphi = 3mm$ pin-fin heat sink filled with PCM has the best thermal performance, the Figures 11a-11b show the comparison of enhancement in time for different volume fractions of PCM to reach SPTs of 60°C and 70°C respectively. It is seen that, maximum time is achieved in case of $\psi = 1.0$, as expected either for SPT of 60°C or 70°C.

Table 5-Time (sec) summary sheet to reach for SPTs at $\psi = 1.0$.

Type of Heat Sinks	Time for SPT (60°C)				Time for SPT (65°C)				Time for SPT (70°C)		
q (kW/m ²)	2.0	2.4	2.8	3.2	2.0	2.4	2.8	3.2	2.4	2.8	3.2
No Fin	4345	3355	2155	1710	6285	4630	2910	2305	6845	4575	2930
$\varphi = 2mm$	8045	5220	3920	3135	9270	5895	4345	3690	6585	5000	4070
$\varphi = 3mm$	10290	5410	4445	3425	13035	6025	4980	4135	7665	5610	4625
$\varphi = 4mm$	6770	4645	3770	2905	7990	5590	4315	3590	6260	4870	3995

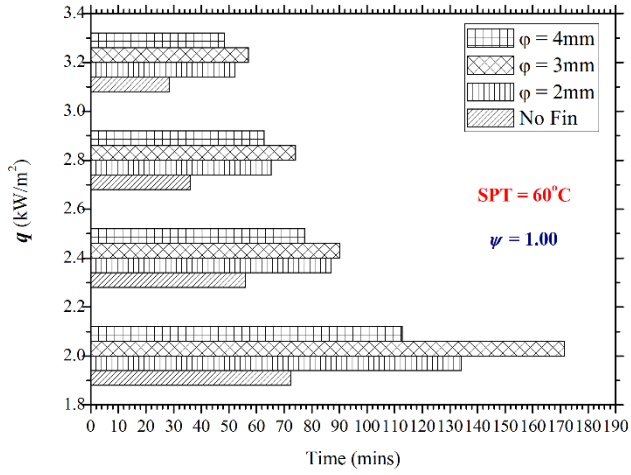


Figure 10(a)

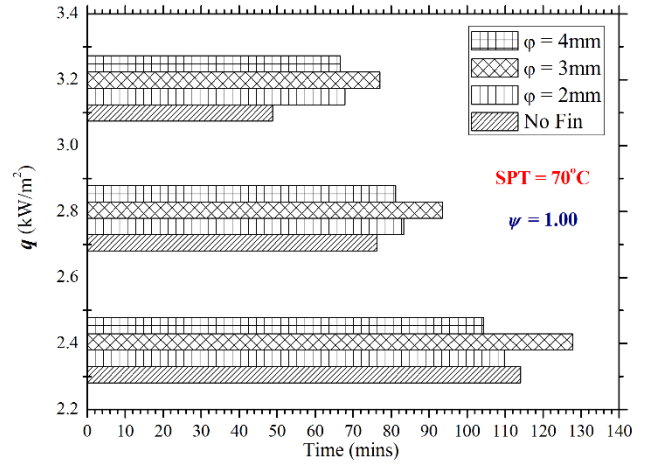


Figure 10(b)

Figure 10- Comparison of enhancement time between various configurations of round pin-fin heat sinks

(a) SPT=60°C (b) SPT = 70°C

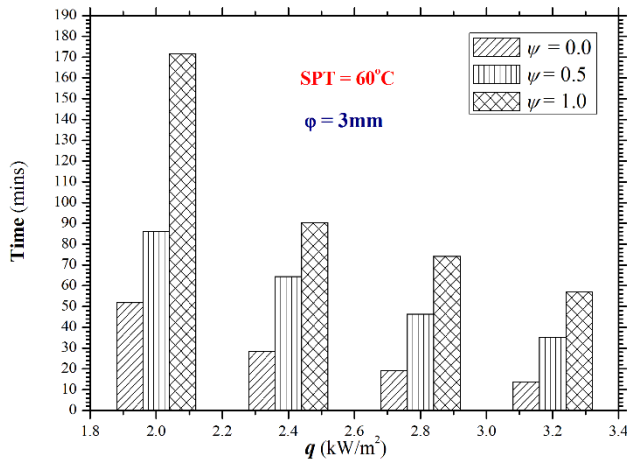


Figure 11(a)

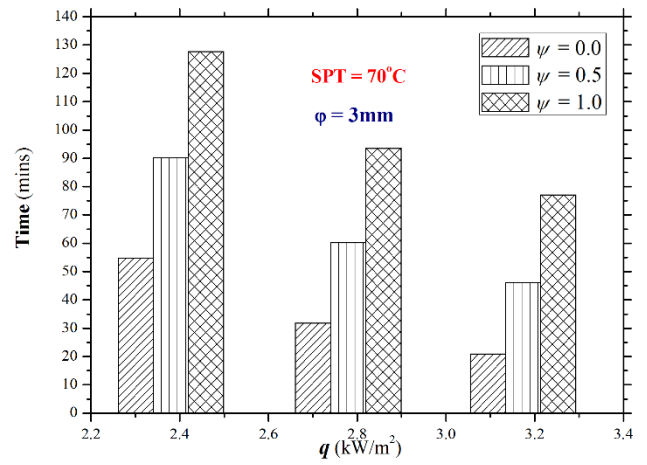


Figure 11(b)

Figure 11- Comparison of enhancement time for different volumetric fraction of PCM of $\phi = 3\text{mm}$ pin-fin heat sink

(a) SPT=60°C (b) SPT = 70°C

3.7-Enhancement ratio with influence of PCM and TCEs

The thermal performance various PCM filled finned heat sinks is carried out by calculating the enhancement ratio for *pin-fin* heat sink against each input heat density. An enhancement ratio with respect to configuration of TCEs, denoted by ξ , is defined as the ratio of at specific volumetric fraction of PCM enhanced finned heat sink to unfinned heat sink. The Eq. 3 is used to calculate the enhancement ratio at PCM of $\psi = 1.0$ for two selective critical SPTs (60°C and 70°C).

$$\xi = \frac{t_{cr_{withTCE}}}{t_{cr_{withoutTCE}}} \quad \text{Eq. 3}$$

The Figures 12a-12b show that the pin diameter of 3mm *pin-fin* heat sink filled with paraffin wax has the higher enhancement ratio at any specific input heat density. A maximum enhancement ratios of 2.4 and 1.6 are obtained is obtain an input density of $2.0kW/m^2$ and $3.2kW/m^2$ for SPT of 60°C and for SPT of 70°C it is 1.6 for an input density of $3.2kW/m^2$. An enhancement ratio, denote by ε , with the influence of with PCM and without PCM, calculating by using Eq. 4, is shown in Figure 13.

$$\varepsilon = \frac{t_{cr_{withPCM}}}{t_{cr_{withoutPCM}}} \quad \text{Eq. 4}$$

Round *pin-fin* heat sink of $\varphi = 3mm$ which evidences the best thermal performance is selected to obtain the enhancement ratio for three critical SPTs of 60°C, 65°C and 70°C. It can be that higher enhancement ratio is achieved for a lower SPT of 60°C at each input heat density. An enhancement ratios of 3.2, 3.9 and 4.2 are obtained for input heat densities of $2.4kW/m^2$, $2.8kW/m^2$ and $3.2kW/m^2$ respectively. The critical SPTs, the temperatures at which any electronic devices can functioned without failure its design constraints, a maximum enhancement ratio is obtained at lower SPT. Additionally, as the input heat density level increases the more enhancement ratio is achieved for any chosen SPTs. The lower enhancement ratio achieved in case of 70°C is due the rapid increase of temperature in post-melting phase. It is concluded that a heat sink filled with PCM are more efficient at higher power densities for passive cooling of electronic equipments.

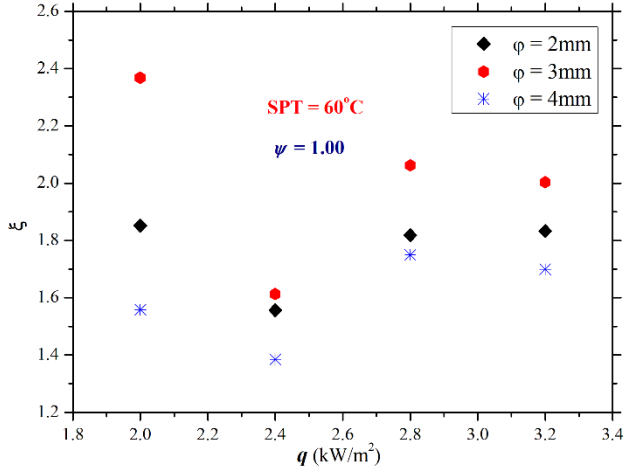


Figure 12(a)

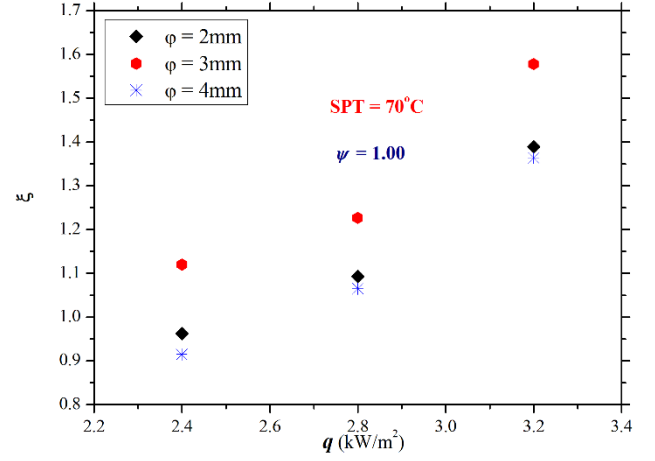


Figure 12(b)

Figure 12- Comparison of enhancement ratios between configurations of round pin-fin heat sinks (a) No fin (b) $\phi = 2\text{mm}$ (c) $\phi = 3\text{mm}$ (d) $\phi = 4\text{mm}$

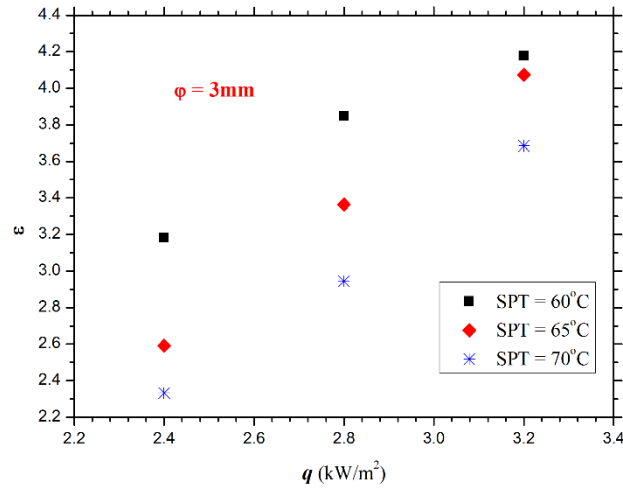


Figure 13- Comparison of enhancement ratios between different SPTs for 3mm pin diameter pin-fin heat sink.

3.8-Effect of heat capacity and thermal conductance

To illustrate the thermal performance of round *pin-fin* heat sinks based on PCM (paraffin wax), specific heat and thermal conductance of each configuration of heat sink is calculated using Eq. 5 and Eq. 6 respectively, given as follows,

$$c = \frac{H}{\Delta T} \quad \text{Eq. 5}$$

$$G = \frac{P}{T_{max} - T_{amb}} \quad \text{Eq. 6}$$

From Figure 14 and 15, it is seen that maximum specific and thermal conductance is achieved in case of $\varphi = 3mm$ *pin-fin* PCM based heat sink. A heat capacity of is $3.1kJ/K$ is obtained this shows a higher thermal energy is needed to raise the heat sink temperature. Thermal conductance actually the rate of heat transfer from the surface of PCM influenced heat sink to surrounding and thermal conductance of $5.7 \times 10^{-1}W/K$ is obtained for $3mm$ pin diameter *pin-fin* PCM based heat sink. An achievement of higher heat capacity and thermal conductance for $\varphi = 3mm$ *pin-fin* PCM based heat sink in comparison of other configured finned heat sink is due to the optimum number of pins, pitch, pin arrangements and pin diameter, which increases the heat transfer rate in surrounding through pins and PCM.

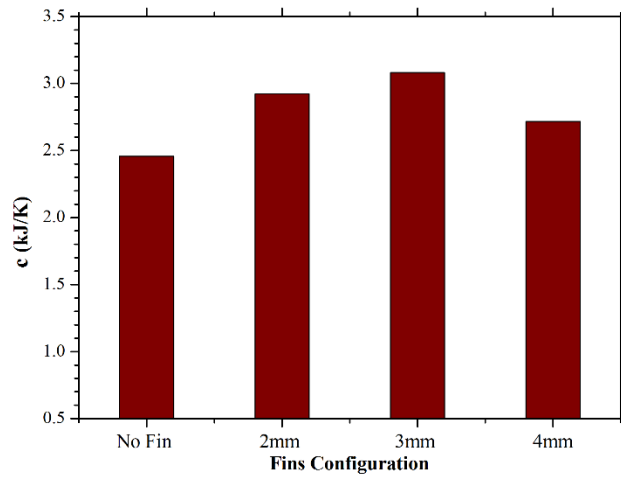


Figure 14-Comparsion of heat capacity for different configurations of round pin-fin heat sinks.

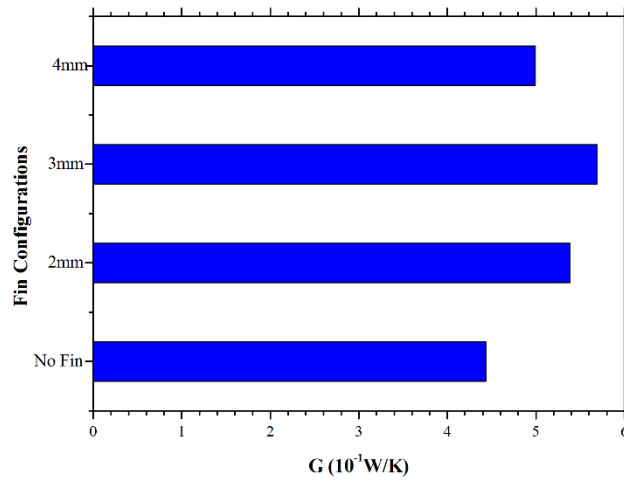


Figure 15-Comparsion of thermal conductance for different configurations of round pin-fin heat sinks.

Conclusions

The present experimental study with basic objective is the parametric analysis of HSU containing round *pin-fin* heat sinks as a TCE filled with PCM (paraffin wax) for efficient TM of portable electronic devices. A constant volume fraction of TCE $\gamma = 9\%$ was chosen and three different volumetric fractions of paraffin wax were taken for input power densities of $1.6kW/m^2$ to $3.2kW/m^2$ with a step of $0.4kW/m^2$. The results reveal a clear picture that a round *pin-fin* heat sinks have a tremendous capability for passive TM of electronic equipments. Some contributions from this analysis are as following;

1. It is concluded that a heat sink with volumetric fraction of $\psi = 1.0$ means fully filled with PCM has more tendency to keep the base temperature in lower comfortable temperature limits than that of $\psi = 0.0$ or $\psi = 0.5$.
2. At low input heat densities the PCM filled HSU are so efficient for passive cooling of electronic devices, because it takes more time to phase change occurs.
3. It is concluded that HSU with pin diameter of 3mm *pin-fin* heat sink filled at $\psi = 1.0$ is more efficient and has significant thermal performance in comparison of 2mm and 4mm *pin-fin* diameter heat sinks.
4. A uniform temperature distribution is found between TCEs through PCM (paraffin wax) which ensures equally melt fraction of PCM in spatial direction.
5. A maximum enhancement in operation time is evidenced for case of $\varphi = 3mm$ *pin-fin* PCM based heat sink either to reach SPTs of 60°C or 70°C for each input heat density.
6. It is concluded that more enhancement ratio is obtained for both critical SPTs of 60°C and 70°C in case of 3mm pin diameter *pin-fin* heat sink in comparison of 2mm and 4mm round *pin-fin* heat sinks.
7. A maximum enhancement ratio of 2.4 is obtained an input heat density of $2.0kW/m^2$ for SPT of 60°C on the bases of TCEs and enhancement ratios of 3.2, 3.9 and 4.2 are calculated at input heat densities of $2.4kW/m^2$, $2.8kW/m^2$ and $3.2kW/m^2$ respectively for a SPT of 60°C on the bases of influence of PCM.
8. Finally, analysis of heat capacity and thermal conductance evidence that a round *pin-fin* PCM filled heat sink of pin diameter of 3mm has maximum heat capacity and thermal

conductance of $3.1\text{kJ}/\text{K}$ and $5.7 \times 10^{-1}\text{W}/\text{K}$ respectively in comparison of 2mm and 4mm pin diameter round *pin-fin* heat sinks.

References

1. Kadam, S.T. and R. Kumar, *Twenty first century cooling solution: Microchannel heat sinks*. International Journal of Thermal Sciences, 2014. **85**: p. 73-92.
2. Kheirabadi, A.C. and D. Groulx, *Cooling of server electronics: A design review of existing technology*. Applied Thermal Engineering, 2016. **105**: p. 622-638.
3. Castell, A. and C. Solé, *11 - Design of latent heat storage systems using phase change materials (PCMs) A2 - Cabeza, Luisa F*, in *Advances in Thermal Energy Storage Systems*. 2015, Woodhead Publishing. p. 285-305.
4. Sahoo, S.K., M.K. Das, and P. Rath, *Application of TCE-PCM based heat sinks for cooling of electronic components: A review*. Renewable and Sustainable Energy Reviews, 2016. **59**: p. 550-582.
5. Nkwetta, D.N. and F. Haghighat, *Thermal energy storage with phase change material—A state-of-the art review*. Sustainable Cities and Society, 2014. **10**: p. 87-100.
6. Casini, M., *5 - Phase-change materials*, in *Smart Buildings*. 2016, Woodhead Publishing. p. 179-218.
7. Wang, X.-Q., C. Yap, and A.S. Mujumdar, *A parametric study of phase change material (PCM)-based heat sinks*. International Journal of Thermal Sciences, 2008. **47**(8): p. 1055-1068.
8. Qu, Z.G., et al., *Passive thermal management using metal foam saturated with phase change material in a heat sink*. International Communications in Heat and Mass Transfer, 2012. **39**(10): p. 1546-1549.
9. Mahrous, A., *THERMAL PERFORMANCE OF PCM-BASED HEAT SINKS*. International Journal of Mechanical Engineering. **2**(4).
10. Grujicic, M., C.L. Zhao, and E.C. Dusel, *The effect of thermal contact resistance on heat management in the electronic packaging*. Applied Surface Science, 2005. **246**(1–3): p. 290-302.
11. Hajmohammadi, M.R., et al., *Evolution in the Design of V-Shaped Highly Conductive Pathways Embedded in a Heat-Generating Piece*. Journal of Heat Transfer, 2015. **137**(6): p. 061001-061001-7.

12. Reza Hajmohammadi, M., et al., *Improvement of Forced Convection Cooling Due to the Attachment of Heat Sources to a Conducting Thick Plate*. Journal of Heat Transfer, 2013. **135**(12): p. 124504-124504-4.
13. Hajmohammadi, M.R., *Reply to: Comments on "Detailed analysis for the cooling performance enhancement of a heat source under a thick plate" by Hajmohammadi et al.* Energy Conversion and Management, 2016. **129**(Supplement C): p. 52-53.
14. Hajmohammadi, M., et al., *Constructal placement of unequal heat sources on a plate cooled by laminar forced convection*. International Journal of Thermal Sciences, 2012. **60**: p. 13-22.
15. Hajmohammadi, M., et al., *Heat transfer improvement due to the imposition of non-uniform wall heating for in-tube laminar forced convection*. Applied Thermal Engineering, 2013. **61**(2): p. 268-277.
16. Najafi, H., B. Najafi, and P. Hoseinpoori, *Energy and cost optimization of a plate and fin heat exchanger using genetic algorithm*. Applied Thermal Engineering, 2011. **31**(10): p. 1839-1847.
17. Baby, R. and C. Balaji, *Experimental investigations on phase change material based finned heat sinks for electronic equipment cooling*. International Journal of Heat and Mass Transfer, 2012. **55**(5-6): p. 1642-1649.
18. Baby, R. and C. Balaji, *Thermal optimization of PCM based pin fin heat sinks: An experimental study*. Applied Thermal Engineering, 2013. **54**(1): p. 65-77.
19. Jaworski, M., *Thermal performance of heat spreader for electronics cooling with incorporated phase change material*. Applied Thermal Engineering, 2012. **35**: p. 212-219.
20. Tigner, J., et al., *Analysis of a platform for thermal management studies of microelectronics cooling methods*. Applied Thermal Engineering, 2013. **60**(1-2): p. 88-95.
21. Baby, R. and C. Balaji, *Thermal performance of a PCM heat sink under different heat loads: An experimental study*. International Journal of Thermal Sciences, 2014. **79**: p. 240-249.
22. Sun, X., et al., *A study on the use of phase change materials (PCMs) in combination with a natural cold source for space cooling in telecommunications base stations (TBSs) in China*. Applied Energy, 2014. **117**: p. 95-103.

23. Alshaer, W.G., et al., *Numerical investigations of using carbon foam/PCM/Nano carbon tubes composites in thermal management of electronic equipment*. Energy Conversion and Management, 2015. **89**: p. 873-884.
24. Alshaer, W.G., et al., *Thermal management of electronic devices using carbon foam and PCM/nano-composite*. International Journal of Thermal Sciences, 2015. **89**: p. 79-86.
25. Fan, L.-W., et al., *Transient performance of a PCM-based heat sink with high aspect-ratio carbon nanofillers*. Applied Thermal Engineering, 2015. **75**: p. 532-540.
26. Kalbasi, R. and M.R. Salimpour, *Constructal design of phase change material enclosures used for cooling electronic devices*. Applied Thermal Engineering, 2015. **84**: p. 339-349.
27. Nada, S.A. and W.G. Alshaer, *Comprehensive parametric study of using carbon foam structures saturated with PCMs in thermal management of electronic systems*. Energy Conversion and Management, 2015. **105**: p. 93-102.
28. Srikanth, R., P. Nemani, and C. Balaji, *Multi-objective geometric optimization of a PCM based matrix type composite heat sink*. Applied Energy, 2015. **156**: p. 703-714.
29. Ahmed, T., et al. *Experimental Investigation of Thermal Management of Tablet Computers using Phase Change Materials (PCMs)*. in *Proc. of the ASME 2016 Summer Heat Transfer Conference*. 2016.
30. Fan, L.-W., et al., *Transient performance of a thermal energy storage-based heat sink using a liquid metal as the phase change material*. Applied Thermal Engineering, 2016. **109**, **Part A**: p. 746-750.
31. Sahoo, S.K., P. Rath, and M.K. Das, *Numerical study of phase change material based orthotropic heat sink for thermal management of electronics components*. International Journal of Heat and Mass Transfer, 2016. **103**: p. 855-867.
32. Swaminathan Gopalan, K. and V. Eswaran, *Numerical investigation of thermal performance of PCM based heat sink using structured porous media as thermal conductivity enhancers*. International Journal of Thermal Sciences, 2016. **104**: p. 266-280.
33. Thomas, J., et al., *Thermal Performance Evaluation of a Phase Change Material Based Heat Sink: A Numerical Study*. Procedia Technology, 2016. **25**: p. 1182-1190.
34. Tomizawa, Y., et al., *Experimental and numerical study on phase change material (PCM) for thermal management of mobile devices*. Applied Thermal Engineering, 2016. **98**: p. 320-329.

35. Wang, H., et al., *Experimental investigation on the thermal performance of a heat sink filled with porous metal fiber sintered felt/paraffin composite phase change material*. Applied Energy, 2016. **176**: p. 221-232.
36. Alimohammadi, M., et al., *Experimental investigation of the effects of using nano/phase change materials (NPCM) as coolant of electronic chipsets, under free and forced convection*. Applied Thermal Engineering, 2017. **111**: p. 271-279.
37. Gharbi, S., S. Harmand, and S.B. Jabrallah, *Experimental study of the cooling performance of phase change material with discrete heat sources – Continuous and intermittent regimes*. Applied Thermal Engineering, 2017. **111**: p. 103-111.
38. Srikanth, R. and C. Balaji, *Experimental investigation on the heat transfer performance of a PCM based pin fin heat sink with discrete heating*. International Journal of Thermal Sciences, 2017. **111**: p. 188-203.
39. Arshad, A., et al., *Thermal performance of phase change material (PCM) based pin-finned heat sinks for electronics devices: Effect of pin thickness and PCM volume fraction*. Applied Thermal Engineering, 2017. **112**: p. 143-155.
40. Ali, H.M. and A. Arshad, *Experimental investigation of n-eicosane based circular pin-fin heat sinks for passive cooling of electronic devices*. International Journal of Heat and Mass Transfer, 2017. **112**: p. 649-661.
41. Ashraf, M.J., et al., *Experimental passive electronics cooling: Parametric investigation of pin-fin geometries and efficient phase change materials*. International Journal of Heat and Mass Transfer, 2017. **115, Part B**: p. 251-263.
42. Put, S., et al., *Die sink electrodischarge machining of zirconia based composites*. British ceramic transactions, 2001. **100**(5): p. 207-213.
43. EMD Millipore is a part of Merck KGaA, D., Germany. 2016; Available from: http://www.emdmillipore.com/US/en/product/Histosec-pastilles,MDA_CHEM-111609.
44. Taylor, B.N. and C.E. Kuyatt, *Guidelines for evaluating and expressing the uncertainty of NIST measurement results*. 1994: US Department of Commerce, Technology Administration, National Institute of Standards and Technology Gaithersburg, MD.